IOP Conf. Series: Materials Science and Engineering **218** (2017) 012011 doi:10.1088/1757-899X/218/1/012011

Studies into the impact of mechanical activation on optimal sintering temperature of UFG heavy tungsten alloys

A V Nokhrin[1], V N Chuvil'deev[1], M S Boldin[1], N V Sakharov[1], G V Baranov[2], A A Popov[1], E A Lantcev[1], V Yu Belov[2] and E S Smirnova[1]

[1] Lobachevsky State University of Nizhny Novgorod, 23 Gagarin Ave., Nizhny Novgorod, 603950, Russia.
[2] Russian Federal Nuclear Center All-Russian Research Institute of Experimental Physics, 37 Mira Ave., Sarov, Nizhny Novgorod region, 607188, Russia

E-mail: nokhrin@nifti.unn.ru

Abstract. The paper dwells on the research conducted into sintering mechanisms, the structure and mechanical properties of ultrafine-grained heavy tungsten W-Ni-Fe alloys. The dependence of alloy density on temperature of sintering (T_{sint}) is found to be nonmonotonic with a maximum equivalent to the optimal sintering temperature. Studies also encompassed the impact that the size of tungsten particles may have on the optimal T_{sint}. An increase in time of mechanical activation (MA) and acceleration of grinding bodies accompanied by a decrease in alloy particle size and formation of non-equilibrium solid solutions is shown to reduce the optimal T_{sint} of alloys. High-energy MA and Spark Plasma Sintering methods were applied to obtain samples of tungsten alloys with high mechanical properties: macroelasticity limit of up to 2,250 MPa, yield strength of up to 2,500 MPa.

1. Introduction

Heavy tungsten alloys are materials with limited mutual solubility that are of great interest both in terms of their applications and as unique objects to study the effect of interfacial and grain boundaries on physico-chemical and physico-mechanical properties of materials.

Currently, the most common method used to produce sizeable pieces from W-Ni-Fe alloys is sintering in hydrogen (HS) at temperatures higher than the melting temperature of the most fusible alloy phase - liquid phase sintering [1, 2].

Tungsten alloys obtained through liquid phase sintering have a coarse-grained heterogeneous structure and, consequently, low mechanical properties: yield strength of sintered W-Ni-Fe alloys with tungsten content of 90-95 wt% does not exceed 1,000 MPa [3, 4]. This factor significantly limits applicability of these materials in construction elements which shall meet high strength requirements.

In this context, of utmost interest is solid-phase sintering of refractory tungsten-based alloys and improved mechanical properties due to the formation of ultrafine-grained (UFG) structures.

The Spark Plasma Sintering (SPS) is considered an advanced method applied to obtained materials with high-density UFG structures [5-8].

The goal of the paper is to study the mechanisms of sintering high-strength W-Ni-Fe alloys and particularly focus on the impact that the size of tungsten particles and regimes of mechanical activation (MA) have on the optimal temperature of sintering of heavy tungsten alloys.

2. Materials. Experimental techniques

Alloys were produced using tungsten powder with average particle size of 3.9 μm, nickel powder with average particle size under 20 μm, iron powder with average particle size under 11 μm and cobalt powder with particle size under 45 μm.

Sintering powders were prepared by adding to the original coarse-grained formula of ultrafine W-Ni-Fe powders obtained though DC arc plasma synthesis (samples of series No.1), low-energy MA (samples of series No.2) and high-energy MA (samples of series No.3, 4) of coarse-grained W-Ni-Fe powders compositions (see Table 1).

The obtained powders were sintered using the method of sintering in hydrogen (HS) (series No.1-3) and Spark Plasma Sintering (SPS) (series No.4).

Low-energy MA (acceleration of grinding bodies equaling 0.4g, where g stands for gravitational acceleration) was performed in a ball mill MV0-10. High-energy MA was performed in a planetary mill APF-3 with acceleration of grinding bodies equaling 60g (rotation rate V_{Ma}=1450 rpm).

HS of samples was performed in a standard resistance furnace in a two-stage mode: heating at 25°/min to 950°C, equalizing at this temperature for two hours, heating at V_h=5°/min to reach the sintering temperature. Powder samples of series No.4 were sintered through SPS using a sintering plant Dr.Sinter model SPS-625 in vacuum (6 Pa). Sintering temperatures varied in the range from 900°C to 1300°C. The temperature was measured with a pyrometer focused on the outside of the graphite mold. Samples were heated with current impulses: current impulse time reaching 3.3 ms. Sintering rate ranged from 50 to 300°/min. Samples were sintered under pressure of 50-70 MPa.

The structure of sintered alloys was studied with an optical microscope Leica IM DRM and scanning electron microscope Jeol JSM-6490. The density of samples was measured using the hydrostatic weighing method in distilled water using Sartorius CPA scales.

To study the mechanical properties of sintered samples, we applied the relaxation tests method to determine in compression tests such values as macroelasticity limit σ_o and yield strength σ_y [9]. The Hall-Petch coefficient (K) was calculated by formula: $K=(\sigma_y-\sigma_o)d^{-1/2}$.

Table 1. Materials and preparation modes.

No.	Alloy (wt.%)	Average size of tungsten particles (μm)		MA mode	Sintering mode
		Initial state	After MA		
1	95%W-3.5%Ni-1.0%Fe-0.5%Co	0.12-0.20	~0.1-0.15	Low-energy MA (0.4g, t_{MA}=72 h, V_{MA}=100 rpm)	HS (V_h=5 °/min, sintering temperature T_{sint}=1200-1500°C)
2	95%W-3.5%Ni-1.0%Fe-0.5%Co	3.9	~1.0	Low-energy MA (0.4g, t_{MA}=5 h, V_{MA}=46 rpm)	HS (V_h=5°/min, T_{sint}=1200-1500°C)
3	95%W-3.5%Ni-1.5%Fe	3.9	0.1	High-energy MA (60g, t_{MA}=20 min, V_{MA}=1450 rpm)	HS (V_h=5°/min, T_{sint}=1200-1500°C)
4	95%W-3.5%Ni-1.5%Fe	3.9	0.1	High-energy MA (60g, t_{MA}=20 min, V_{MA}=1450 rpm)	SPS (V_h=50-300°/min, T_{sint}=900-1300°C)

3. Experimental results

Figure 1a shows the dependence of density of 95W-3.5Ni-1.0Fe-0.5Co alloy on HS temperature. The dependence of density (ρ) of 95W-3.5Ni-1.0Fe-0.5Co alloy added with 10% of UFP mixture on sintering temperature is three-stage. The first stage sees monotonic growth in the alloy density from 15.77 to 17.77 g/cm^3 (from 87.1% to 98.2% of the theoretical density ρ_{th}) as temperature of sintering (T_{sint}) rises from 1200°C to T_1=1400°C. However when the T_{sint} reaches T_2~1450°C, there is a slight decrease in density to 17.53 g/cm^3 (to 96.85%). Further increase in T_{sint} to 1500°C ensures density growth to17.67 g/cm^3 (97.6% of the theoretical alloy density, see Table 1, Fig. 1a). Similar dependencies $\rho(T_{sint})$ were obtained for alloys added with 20% UFP, 100% UFP alloys are similar in nature.

It shall be noted that the above dependencies $\rho(T_{sint})$ differ from any dependences obtained while sintering coarse-grained powders (see Fig. 1a): dependence $\rho(T_{sint})$ for such materials is monotonic in nature with maximum density reached at T_{sint} corresponding to the melting point of γ-phase.

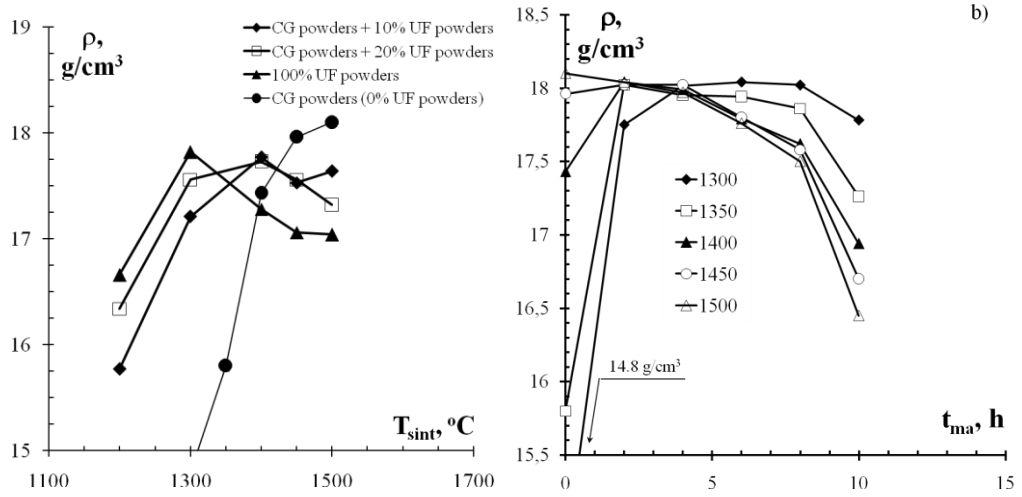

Figure 1. Dependence of density in samples of series No.1 (a) and series No.2 (b) exposed to low-energy mechanical activation on HS temperature.

It shall be also noted that the effect of density reduction at the second sintering stage (at $T_1 \leq T_{sint} \leq T_2$) is not connected with the growth of porosity in the alloy – detailed metallographic and electron microscopic studies revealed no change in the volume ratio of pores – 95W-3.5Ni-1.0Fe-0.5Co alloy samples after sintering have a high density homogeneous structure with density reaching 17.73-17.82 g/cm^3 after sintering at T_1, which approximates 98.0-98.5% of the theoretical alloy density.

Research into mechanical properties of 95W-3.5Ni-1.0Fe-0.5Co alloys in a variety of structural states shows that increase in the UFP volume ratio from 10% to 100% in alloys sintered at optimal temperature T_1 leads to greater σ_o rising from 230 MPa to 635 MPa and greater σ_y rising from 655 MPa to 905 MPa (see Table 2). Curiously enough, the Hall-Petch coefficient (K) decreases with the increase in the grain size in alloys (see Table 1).

Table 2. Impact of ultrafine powder (UFP) additives on optimal sintering temperature, density and mechanical properties of a 95W-3.5Ni-1.0Fe-0.5Co alloy (series No.1)

UFP ratio in alloys (%)	Representative sintering temperatures		Alloy density at optimal sintering temperature T_1		Average grain size	Mechanical properties of alloys		
	T_1 (°C)	T_2 (°C)	ρ (g/cm^3)	ρ (%)	d (μm)	σ_o (MPa)	σ_y (MPa)	K (MPa·m$^{1/2}$)
0	1450	1500	18.02	99.6	22	-	635	-
10	1400	1450	17.77	98.2	15	230	655	1.6
20	1350-1400	1450	17.73	98.0	10	240	665	1.3
100	1300	1450	17.82	98.5	4	635	905	0.5

The dependence of alloy series No.2 density on temperature of sintering $\rho(T_{sint})$ is found to be nonmonotonic which is similar to the dependence $\rho(T_{sint})$ for samples of series No.1 (see Fig.1b).

It should be noted that the dependence $\rho(T_{sint})$ is also influenced by mechanical activation time (t_{MA}): an increase in t_{MA} from 2 to 10 hours leads to a decrease in density of alloys sintered at T_{sint}=1500°C from 18.02 to 16.45 g/cm^3. It has been observed that as well as with samples of series

No.1, structural research revealed no increase in the volume ratio of pores at the second sintering stage at $T_1 \leq T \leq T_2$.

Table 3. Impact of low-energy MA time on optimal sintering temperature and structure of 95W-3.5Ni-1.0Fe-0.5Co alloy (series No.2)

t_{ma} (h)	Optimal temperature	Alloy density at optimal sintering temperature $T_{sint}=T_1$		Average grain size	Mechanical properties of alloys		
	T_1, (°C)	ρ (g/cm^3)	ρ (%)	d (μm)	σ_o (MPa)	σ_y (MPa)	K (MPa·m$^{1/2}$)
0	1450-1500	18.08-18.10	100	50-70	-	-	-
2	1450	18.02-18.05	99.6-99.7	50	280	550	1.9
4	1400	18.00	99.5	36-38	300	550	1.5-1.6
6	1350	17.95-18.00	99.2-99.5	15-20	320	590	1.0-1.2
8	1300	17.97	99.3	5-10	740	930	0.4-0.6
10	≤1300	17.78	98.2	3-5	780	1000	0.4-0.5

The dependence of average tungsten particle size and alloy density after high-energy MA (series No.3) on sintering temperature is shown on Fig. 2a. The above data prove that an increase in alloy heating temperature above optimal sintering temperature T_1 leads to accelerated grain growth: with alloys sintered at T_{sint}=1100°C and 1450°C, the average grain size is 1.5 and 22 μm respectively, which is an order of magnitude bigger than the average size of tungsten particles in the original state.

The dependence $\rho(T_{sint})$ of a 95W-3.5Ni-1.5Fe alloy is similar to analogous dependences for alloys of series No.1 and No.2 and has two stages (Fig. 2a). As before, within the T_{sint} range from 1350°C to 1450°C corresponding to the effect of density reduction (see above), detailed electron microscopic and metallographic studies revealed no increase in the volume ratio of pores: materials sintered at T_{sint}=1350°C have a high-density structure with the volume ratio of pores not exceeding 0.2%.

Dependencies of σ_o and σ_y in a 95W-3.5Ni-1.5Fe alloy (series No.3) on temperature of sintering are two-stage; maximal mechanical properties (σ_o=1030 MPa, σ_y=1320 MPa) are ensured in an alloy sintered at T_{sint}=1250°C. Further T_{sint} increase leads to reduced material strength caused by recrystallization processes. Similar to samples of series No.1 and 2, the Hall-Petch coefficient decreases while the average grain size in alloys grows.

Figure 2c shows dependencies $\rho(T_{sint})$ of 95W-3.5Ni-1.5Fe alloy (series No.4) density obtained through high-energy MA and SPS. The presented results allow to generalize that the optimal T_{sint} for 95W-3.5Ni-1.5Fe alloy approximates T_1~1100°C (V_h=100°/min). Reduction in the heating rate causes a shift in the optimal sintering temperature to higher values: optimal temperature of sintering for SPS alloys heated at the rate of 50°/min is T_1=1200°C.

Research into the structure of samples after high-energy MA and SPS show that the structure with average grain size of ~500 nm is formed in alloys at temperature T_1=1100°C.

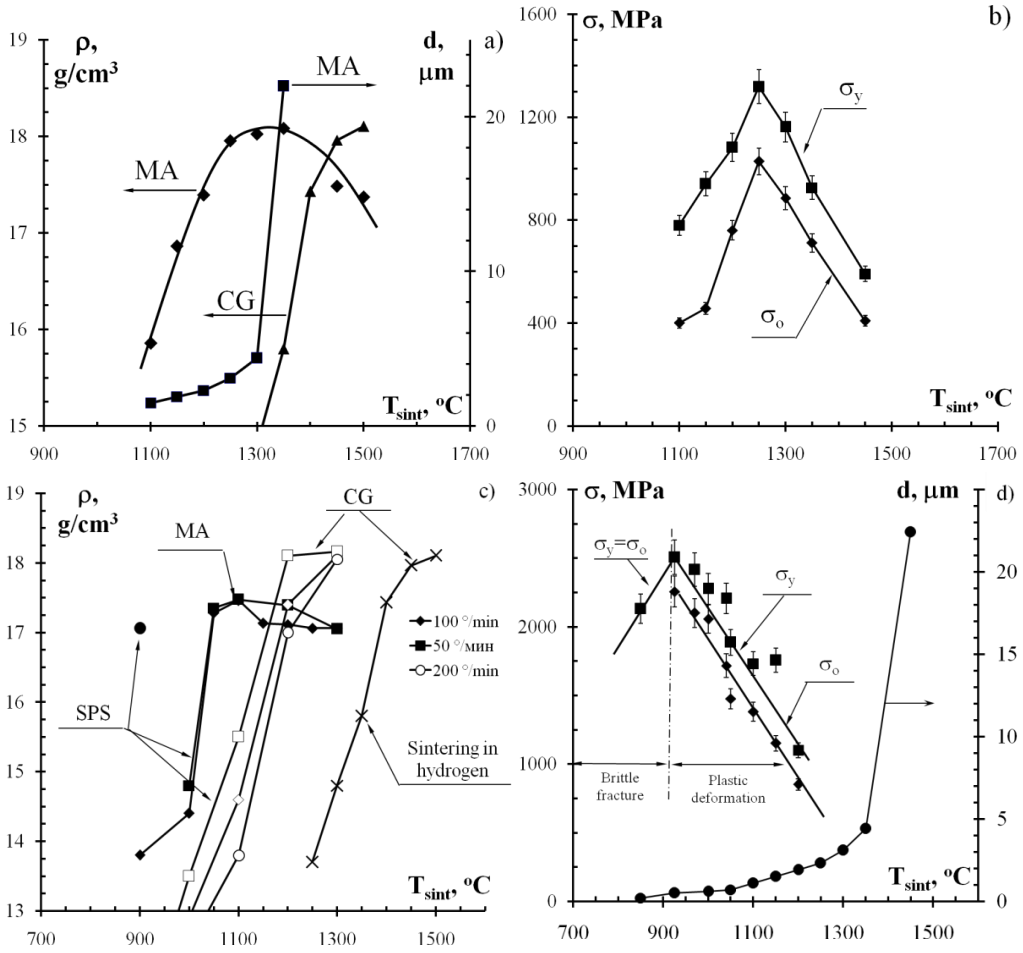

Figure 2. Dependence of density (a, c), mechanical properties and grain size (b, d) on HS temperature (a, b) and SPS temperature (c, d) of 95W-3.5Ni-1.5Fe alloy exposed to high-energy MA.

Figure 2d presents graphs showing the dependence of mechanical properties found with a 95W-3.5Ni-1.5Fe alloy (series No.4) on T_{sint} at the heating rate of 100°/min. Maximal mechanical properties of alloys (σ_o=2250 MPa, σ_y=2500 MPa) are ensured through heating at the rate of 100°/min at T_{sint}=925-950°C. However it should be noted that ductility (in compression tests) of alloys exposed to such a sintering mode is small and does not exceed 0.2-0.5%. Although SPS at higher temperatures (T_{sint}>1050°C) reduces strength properties of alloys ($\sigma_o \leq$1500 MPa, $\sigma_y \leq$ 1900 MPa), it ensures higher ductility: alloy samples are resistant to deterioration after ~10% contraction.

Values of the Hall-Petch coefficient in UFG alloys obtained using SPS appear to be much less than in fine-grained and coarse-grained alloys obtained though sintering in hydrogen (0.1-0.3 MPa·$m^{1/2}$).

4. Analysis of experimental data

4.1 Impact of MA on the dependence of density on sintering temperature

Experimental studies have shown that the dependence of samples density on the sintering temperature is three-stage in nature and has its maximum corresponding to optimal sintering temperature T_1. This result was unexpected as dependence of density on sintering temperature for common coarse-grained W-Ni-Fe alloys is monotonic.

The first rising branch of $\rho(T_{sint})$ dependence obviously reflects the accelerated process of diffusion mass transfer of tungsten in γ-phase at rising temperatures, while its behavior is rather typical of

sintering of coarse-grained W-Ni-Fe mixtures. However the reason for significant density reduction – more than by 7% – at the second stage requires extra explanation.

Let us consider deformation behavior of W-Ni-Fe mixture during mechanical activation. During mechanical activation, deformation dissolution of tungsten ions in nickel-based γ-phase occurs. It shall be noted that increased MA time and acceleration of grinding bodies during mechanical activation are sure to enhance the degree of non-equilibrium in the solid tungsten solution in γ-phase.

While heating, the system tends to reduce its internal energy by means of diffusion mass transfer of excess concentration of tungsten ions from the FCC lattice of γ-phase to the particles of α-phase (tungsten), as this decreases the degree of supersaturation for nonequilibrium solid tungsten solution in nickel-based γ-phase. This process decreases density to its equilibrium value at the second stage of sintering (at $T_1<T\sim0.7T_m<T_2$) alloys (where T_m is the melting temperature of γ-phase). Further increase in alloy density at higher sintering temperatures is caused by accelerated diffusion mass transfer at elevated sintering temperature which is exponential in nature.

Thus, the reason for decreased density at the second sintering stage ($T_1<T_{sint}<T_2$) of mechanically activated tungsten alloys lies in intensive diffusion drift of tungsten atoms away from the nickel-based phase. This conclusion fully conforms to the results presented in paper [10] which showed that an increase in sintering temperature of mechanically activated 90W-7Ni3Fe alloy from 1250°C to 1400°C went along with a decrease in concentration of tungsten in γ-phase from ~50% to 36-38%.

4.2 Impact of MA on tungsten alloy strength

The analysis of results obtained from studying mechanical properties shows that the dependence of σ_y on grain size d in σ_y-$1/d^{1/2}$ coordinates may be interpolated by a straight line (see Fig. 3a). This means that for the alloys under study the following Hall-Petch relation is true: $\sigma_y=\sigma_o+K\cdot d^{-1/2}$.

It shall be noted that with an increase in grain size in sintered alloys we observe bigger K coefficient (see Fig. 3b). Minimal K values (~0.1-0.3 MPa·$m^{1/2}$) are found in alloys obtained though SPS with minimal grain growth (α-W particles grow from the initial size of ~0.1 μm to 0.95-1.1 μm). Maximal K values (~1.6-1.9 MPa·$m^{1/2}$) are observed in alloys of series No.3 that experience sizable grain growth (from the original particles size of ~1 μm to 50 μm) while sintering.

In our opinion, bigger grain boundary contribution (increased K coefficient) during grain growth results from supersaturated solid tungsten solution in γ-phase. An interfacial (α-γ)-boundary migrating at high rate 'sweeps' tungsten atoms in γ-phase. This leads to a thin layer of heavily supersaturated solid tungsten solution in γ-phase that is formed in front of a migrating (α-γ)-boundary. This layer contributes to strength (increased K value) and may partly compensate for reduced alloy strength arising from grain growth.

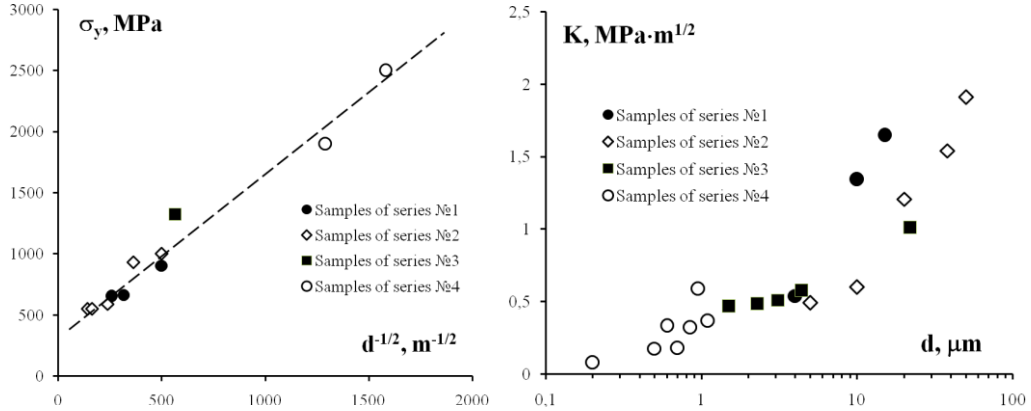

Figure 3. Dependence of yield strength σ_y on grain size (a) and dependence of Hall-Petch coefficient (K) on grain size for tungsten alloys (b)

5. Conclusion

Experimental research was conducted into the structure of mechanically activated nano- and ultrafine tungsten alloys obtained through sintering in hydrogen and SPS. The dependence of alloy density on temperature of sintering is found to be nonmonotonic with a maximum equivalent to optimal temperature of sintering. Increase in MA time and acceleration of grinding bodies during mechanical activation accompanied by decrease in alloy particle size and formation of non-equilibrium solid solutions is shown to reduce optimal temperatures of sintering of alloys.

Nonmonotonic nature of dependence of alloy density on temperature of sintering is shown to be determined by the kinetics of diffusion-controlled processes associated with the changes in tungsten concentrations in nickel-based γ-phase solid solution, as well as development of recrystallization processes at high-temperature heating of alloys.

Formation of a supersaturated solid tungsten solution in γ-phase is found to increase Hall-Petch coefficient and may ensure extra strengthening in case of intensive migration of interfacial boundaries during sintering of tungsten alloys.

Acknowledgements

The research is carried out with the support of the Grant of the President of the Russian Federation No. NSh-7179.2016.8 and Ministry of Education and Science of Russian Federation.

References

[1] Green E C, Jones D J, Pitkin W R 1954. *Symposium of Powder Metallurgy*. *Special Report* (**58)** 253.
[2] Krock R, Shepard H 1963 *Transaction of the Metallurgical Society of AIME* **227** (**5**) 1127.
[3] Gong X, Fan J L, Ding F, Song M, Huang B Y, Tian J M 2011 *Materials Science and Engineering A* **528** 3646.
[4] Das J, Kiran U R, Chakraborty A, Prasad N E 2009 *Int. Journal of Refractory Metals and Hard Materials* **27** 577.
[5] Tokita M 2013 *Spark Plasma Sintering (SPS) Method, Systems, and Applications (Chapter 11.2.3)*. In Handbook of Advanced Ceramics (Second Ed.). Ed. Shigeyuki Somiya, Academic Press. 1149.
[6] Orlova A I, Volgutov V Yu, Mikhailov D A, Bykov D M, Skuratov V A, Chuvil'deev V N, Nokhrin A V, Boldin M S, Sakharov N V 2014 *Journal of Nuclear Materials* **446** (**1-3**) 232.
[7] Chuvildeev V N, Panov D V, Boldin M S, Nokhrin A V, Blagoveshensky Yu V, Sakharov N V, Shotin S V, Kotkov D N 2015 *Acta Astronautica* **109** 172.
[8] Chuvil'deev V N, Boldin M S, Dyatlova Ya G, Rumyantsev V I, Ordan'yan S S 2015 *Inorganic Materials* **51** (**10**) 1047.
[9] Nokhrin A V 2012 *Deformation and Fracture of Materials* (**11)** 23 (in Russian).
[10] Fan J, Huang B, Qu X, Zou Z 2001 *Int. Journal of Refractory Metals and Hard Materials*. **19** 73.